

Stability analysis and simulation of a two DOF robotic system based on linear control system.

Imran S. Sarwar, Afzaal M. Malik

Department of Mechanical Engineering

National University of Sciences and Technology, Rawalpindi, 46000 Pakistan.

Email: imransarwar@ceme.edu.pk, drafzaalmalik@yahoo.com

Abstract- The ability to identify and follow a moving object is not only important for human activities, but it is also critical necessity in the use of robots for automation and manufacturing, security applications, and for life sciences. This achieved by using the pan and tilt mechanism with camera. The paper deals with the stability analysis and simulation of two degree of freedom (DOF) robotic system for positioning or aiming a device based on linear model. The 2-DOF robotic system is formed by combining tilt mechanism with pan mechanism. The stability analysis of the pan and tilt mechanism is performed before designing the motion controllers for the 2-DOF robotic system. The state space model and transfer function of the pan and tilt mechanisms were determined. For this purpose dynamical model of pan and tilt mechanisms was determined by using Newton-Euler equation. To perform the analysis and simulation, all the parameters involved in the system dynamics were identified. The robotic system has two degrees of freedom due to tilt and pan mechanisms. Here tilt mechanism has one revolute joint and pan mechanism has also one revolute joint. The objective of this research work is to derive motion controllers for the pan and tilt mechanisms. These controllers make possible for camera to point in a desired direction within allowable specifications. The lead compensators are used as motion controllers to meet the desired specification. The feedback control system is used with lead compensator for the position control of the pan and tilt mechanism in this paper. The advantage of lead compensator is that it can be implemented using passive network.

I. INTRODUCTION

The schematic of the tilt mechanism has been shown in fig. 1 along with computer aided design (CAD) of tilt mechanism. The tilt mechanism is supporting and orienting the device (camera) in a desired direction. The tilt mechanism is rotatable about a tilt axis supported on the pan mechanism. The tilt motor drives the tilt mechanism. There is a drive pulley on the shaft of the motor. Through the mechanism of pulleys and V-belt, the torque is transferred to the camera platform. This mechanism has one revolute joint (R).

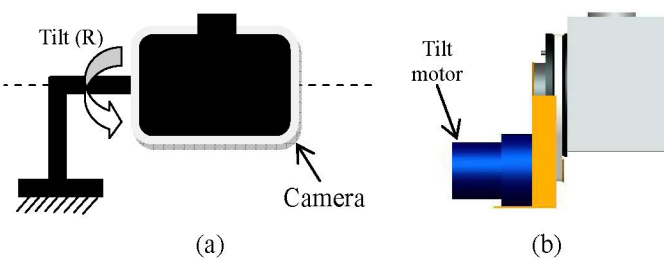


Fig. 1. (a) Schematics and (b) CAD of the tilt mechanism

The schematic of the pan mechanism has one degree of freedom as shown in fig. 2(a). The CAD of pan mechanism is presented in fig. 2(b). The pan mechanism is supporting and orienting the tilt mechanism in the desired direction. The pan mechanism is rotatable about a pan axis. The base plate has rigid joint with vertical supports. It can be fixed on any vehicle such as an aircraft. The pan motor drives the pan mechanism. Similarly, in fig. 2(b), a drive pulley is fixed on the shaft of the motor and another pulley is fixed with the supporting plate. Through this mechanism of pulleys and V-belt, the torque is transferred to the structure as shown in fig. 2.

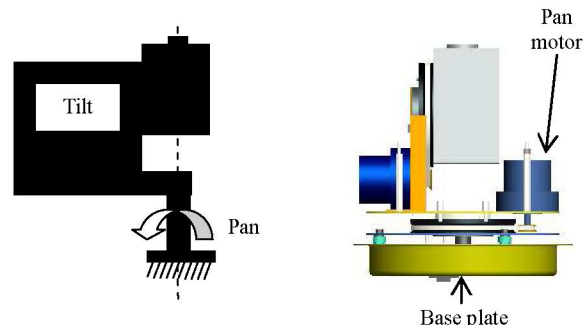


Fig. 2. (a) Schematics and (b) CAD of the pan mechanism

The tilt and pan model used in this paper is based on Newton-Euler equation and is discussed in sections II and IV. The viscous friction was identified from experiments [14]. The mass and inertia are obtained from CAD as explained in section II. The tilt mechanism along with lead compensator is analyzed and simulated in Section III. The pan mechanism along with lead compensator is analyzed and simulated in Section V. Both the motion controllers are designed to achieve the desired response of the robotic system. The allowable specifications are: the settling time expected to be less than 0.5 seconds; the steady state error can be tolerated within $\pm 2\%$ and the %overshoot is expected to be kept below 22%.

When pan and tilt mechanisms are joined together, they form robotic system with two revolute joints (RR) as in fig 2(b). The applications of these mechanisms working together or independently are object tracking i.e. target acquisition, border patrol, search and rescue etc. The results are presented in section VI and compared with robotic system using PD controller from [14] in section VII.

II. TILT MECHANISM

The dynamical model of the tilt mechanism is developed in the II (A). The stability analysis of the tilt mechanism is presented in the II (B). The transfer function of the tilt mechanism is calculated in the section II (C). The tilt mechanism response is discussed in II (D).

A. Linear Model of Tilt Mechanism

The linear model of the tilt mechanism follows from the Newton-Euler equation under certain assumptions. The nonlinear model based on the Newton-Euler equation [1, 3] is as follows.

$$\tau = J_{eff} \ddot{\theta} + f_v \dot{\theta} + f_c \operatorname{sgn}(\dot{\theta}) + mgl \sin \theta \quad (1)$$

Here τ = Torque, J_{eff} = Effective inertial load, f_v = Viscous friction, f_c = Coulomb friction, θ = Angle between the force (mg) and arm length (l).

The effective inertial load of the system is computed from the following relation [14].

$$J_{eff} = \frac{J_a + J_p}{n} + nJ_L \quad (2)$$

J_a = Actuator inertia, J_p = Pulley inertia, J_L = Load inertia, n = ratio between pulleys diameter.

The nonlinear terms in equation (2) are $\operatorname{sgn}(\dot{\theta})$ and $\sin \theta$. These terms with nonlinearity are neglected in the linear model of the system. Thus, the linear model follows from (1) takes the following form

$$\tau = J_{eff} \ddot{\theta} + f_v \dot{\theta} \quad (3)$$

This second-order differential equation can be expressed in state space form by introducing the state variables: $x_1 = \theta$, $x_2 = \dot{\theta}$, with the derivatives as $\dot{x}_1 = \dot{\theta}$, $\dot{x}_2 = \ddot{\theta}$. Thus the state equations are

$$\dot{x}_1 = x_2 \quad (4)$$

$$\dot{x}_2 = -\frac{f_v}{J_{eff}} x_2 + \frac{u}{J_{eff}} \quad (5)$$

The state space model in vector-matrix form is as follows. [9-14]

$$\dot{x} = \begin{bmatrix} 0 & 1 \\ 0 & -\frac{f_v}{J_{eff}} \end{bmatrix} x + \begin{bmatrix} 0 \\ \frac{1}{J_{eff}} \end{bmatrix} u$$

Here

$$x = \begin{bmatrix} x_1 \\ x_2 \end{bmatrix}, \dot{x} = \begin{bmatrix} \dot{x}_1 \\ \dot{x}_2 \end{bmatrix}, u = \tau, A = \begin{bmatrix} 0 & 1 \\ 0 & -\frac{f_v}{J_{eff}} \end{bmatrix}, B = \begin{bmatrix} 0 \\ \frac{1}{J_{eff}} \end{bmatrix}, C = [1 \ 0] \quad (6)$$

The state space model of the tilt mechanism is described by (6). Now we analyze the stability of the tilt mechanism in II (B).

B. Stability Analysis of Tilt Mechanism

The stability analysis of the tilt mechanism based on its equilibrium points is performed in this section. For the above state space equation (4-5) of the tilt mechanism, we have found all the equilibrium points by putting $u = 0$, $\dot{x}_1 = 0$ and $\ddot{x}_2 = 0$ as follows [2]

$$0 = x_2$$

$$0 = -\frac{f_v}{J_{eff}} x_2$$

The equilibrium points are located at the $(x_1, 0)$ where x_1 belongs to the set of real numbers. The function $f(x)$ for the stability analysis of the tilt mechanism follows from (4-5). The type of each isolated equilibrium point can be found using the following function

$$f(x) = \begin{bmatrix} \dot{x}_1 \\ \dot{x}_2 \end{bmatrix} = \begin{bmatrix} x_2 \\ -\frac{f_v}{J_{eff}} x_2 \end{bmatrix} \quad (7)$$

The behavior of the tilt mechanism can be analyzed using (7). The Jacobian of the tilt mechanism given below follows from (7).

$$\frac{\partial f}{\partial x} = \begin{bmatrix} 0 & 1 \\ 0 & -\frac{f_v}{J_{eff}} \end{bmatrix}$$

The Jacobian of the tilt mechanism evaluated at $(x_1, 0)$ is given below

$$A = \left. \frac{\partial f}{\partial x} \right|_{(x_1, 0)} = \begin{bmatrix} 0 & 1 \\ 0 & -\frac{f_v}{J_{eff}} \end{bmatrix}$$

The viscous friction f_v used in the above expression was determined experimentally. The value of viscous friction is 0.00505 Nms/rad. To find the effective inertial loads of tilt system, the inertial load of the tilt mechanism was analyzed in the Pro-E, the pulley inertia was determined separately in Pro-E and the actuator inertia was obtained from the motor datasheet. The effective load of the tilt mechanism is calculated by using equation (2), and is summarized in table I.

TABLE I
INERTIAL LOAD FOR TILT MECHANISM

	J_L (Kg m ²)	J_p (Kg m ²)	J_a (Kg m ²)	n	J_{eff} (Kg m ²)
Tilt mechanism	0.0056	4.4×10^{-7}	1.6×10^{-6}	5.7143	0.0320

Thus the Jacobian matrix determined carefully through experimental investigation is given below

$$A = \begin{bmatrix} 0 & 1 \\ 0 & -0.1578 \end{bmatrix}$$

The eigenvalues corresponding to the Jacobian determined were found as follows

$$|\lambda I - A| = \begin{vmatrix} \lambda & -1 \\ 0 & \lambda + 0.1578 \end{vmatrix} = \lambda^2 + 0.1578\lambda$$

$$\lambda^2 + 0.1578\lambda = 0, \lambda_{1,2} = 0, -0.1578$$

Thus for the equilibrium points, the eigenvalues are at 0 and -0.1578. As one of the eigenvalues of A is zero, the phase portrait is in some sense degenerated [2]. Here the matrix A has a nontrivial null space. All the vectors in the null space of A are equilibrium points for the system. All the trajectories coverage to the equilibrium subspace as $\lambda_2 < 0$.

C. Transfer Function of Tilt Mechanism

The transfer function of the tilt mechanism is found using (6), value of f_v , table I and $G(s) = C(sI - A)^{-1}B$ from [9], and is given below

$$G(s) = \frac{31.2495}{s^2 + 0.1578s} \quad (8)$$

The tilt mechanism is marginally stable as one of the system poles lies at the origin. The transfer function of the tilt mechanism is described by (8).

D. Tilt Mechanism Response

As noticed in [7,14], the (8) has a setting time (50.697 sec) and a steady-state error (12.1401) when the gain (4.160×10^{-4}) is selected on the root locus with radial line. Both the values far exceed the desired performance values. This problem has to be compensated by designing the control system, as explained in the next section.

III. MOTION CONTROL OF TILT MECHANISM

The linear tilt system is controlled by lead compensator as shown in fig. 3. The compensated tilt mechanism (tilt mechanism with lead compensator) analysis and simulation via the root locus method is described below.

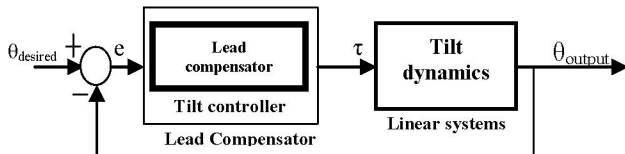


Fig. 3. Tilt feedback control system

The objective of a lead compensator is to drive the T_s to less than 0.5 sec for the unity feedback system shown in fig. 3. The compensated system is schematically shown in fig. 4.

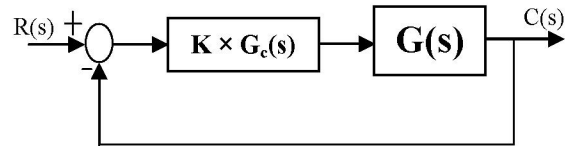


Fig. 4. Closed loop system with compensator

The lead compensator is found by using [9-12]. For the lead compensator, the calculated natural frequency, the desired dominant pole location (DPL) and zero location (z_c) are

$$w_n = 28.9855 \text{ rad/sec}, \quad DPL = -20.0028 + 20.9799i,$$

$$\text{Angle at desired pole} = 92.9499^\circ, z_c = 0.01,$$

$$\text{Angular Contribution by zero} = -46.3471$$

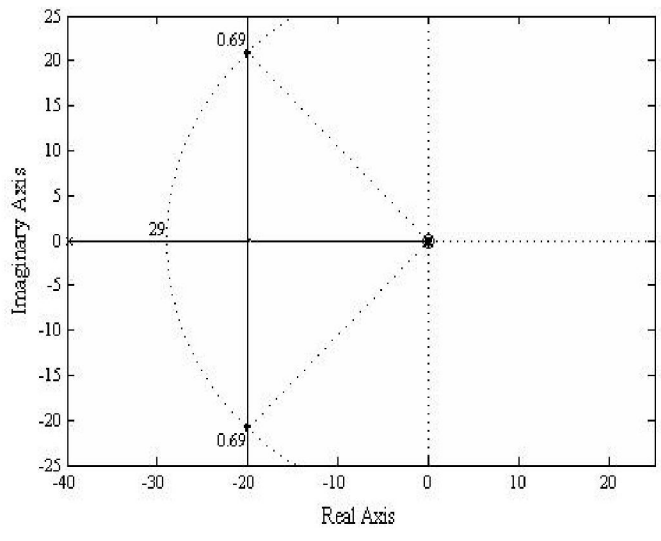
Hence, the compensator angle contribution is 46.57° and thus the lead compensator transfer function may be written as

$$G_c(s) = \frac{s + 0.01}{s + 40.1079} \quad (9)$$

The open-loop transfer function resulting for fig. 4 is determined using (8) and (9), and is given below

$$KG(s)G_c(s) = K \frac{31.2495(s + 0.01)}{s(s + 0.1578)(s + 40.1079)} \quad (10)$$

The open loop transfer function of tilt mechanism with lead compensator was determined in (10). According to the root locus technique [9], it has three branches of root locus, symmetrical with respect to the real axis, real-axis segment is $[0, -0.01]$ and $[-0.1578, -40.1079]$, starting points are the open-loop poles at 0, -0.1578 and -40.1079, ending points are the open-loop zeros at $-0.01, \infty$ (infinity), $-\infty$, real-axis intercept is at -20.128, angle of asymptotes are $90^\circ, 270^\circ$ and breakaway point is at -20.128. The result of root-locus method, based on simulation performed in Matlab is shown in fig. 5 (a).



(a)

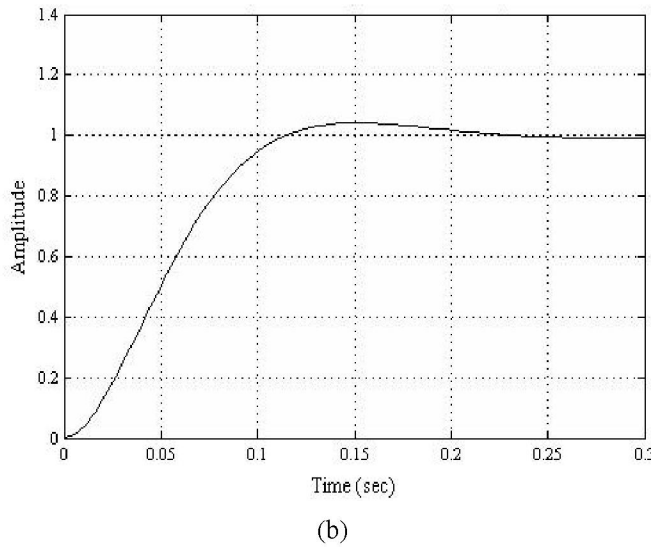


Fig. 5. Compensated system (a) Root locus with radial line (b) step response

A damping ratio of 0.69 is represented by a radial line drawn on the root-locus in fig 5(a). We have found dominant pair of poles at $-19.9889 \pm 20.8851i$ along the damping ratio line for a gain (K) equal to 26.5558. The compensated system step response is shown in fig. 5 (b). The closed loop transfer function ($T(s)$) based on (10) is as follows

$$T(s) = \frac{829.9s + 8.299}{s^3 + 39.99s^2 + 836.1s + 8.299} \quad (11)$$

As noticed in fig. 5(b), the setting time (0.196 sec) and the steady-state error (0.7574) meet the desired performance values.

IV. PAN MECHANISM

The dynamical model of the pan mechanism is developed in the IV (A). The stability analysis based on the state space model of the pan mechanism is presented in the IV (B). The transfer function of the pan mechanism is calculated in the IV (C). The pan mechanism response is discussed in IV (D).

A. Linear Model of Pan Mechanism

The linear model of the pan mechanism follows from the Newton-Euler equation [1] under certain assumptions. The nonlinear model based on the Newton-Euler equation is as follows.

$$\tau = J_{eff}\ddot{\theta} + f_v\dot{\theta} + f_c sgn(\dot{\theta}) + mgl \sin \theta \quad (12)$$

θ = Angle between the force (mg) and arm length (l)

The nonlinear model of pan mechanism presented in [2, 14] can also be used for analysis and simulation. For the pan mechanism $mgl \sin \theta$ term is effectively equal to zero explained by fig. 2. Therefore, (12) becomes

$$\tau = J_{eff}\ddot{\theta} + f_v\dot{\theta} + f_c sgn(\dot{\theta}) \quad (13)$$

This equation is for the pan mechanism and represents the nonlinear model of pan mechanism. This nonlinear equation needs to be linearized in order to develop a controller for the pan mechanism. The nonlinear term in equation (13) is $sgn(\dot{\theta})$. Therefore, term with nonlinearity is neglected in the linear model of the system. Linearization simplifies the pan model. Thus, the linear model takes the following form

$$\tau = J_{eff}\ddot{\theta} + f_v\dot{\theta} \quad (14)$$

The viscous friction has been determined experimentally. Similar to [7,14], the value of the viscous friction is 0.007 Nms/rad for the pan mechanism. The effective load is calculated by using equation (2), and is shown in table II.

TABLE II
INERTIAL LOAD FOR PAN MECHANISM

	J_L ($Kg\ m^2$)	J_m ($Kg\ m^2$)	J_a ($Kg\ m^2$)	n	J_{eff} ($Kg\ m^2$)
Pan mechanism	0.0743	4.4×10^{-7}	1.6×10^{-6}	5.7143	0.4173

The state space model for pan mechanism was developed as in the case of tilt mechanism and is given below in vector-matrix form.

$$\begin{aligned} \dot{x} &= \begin{bmatrix} 0 & 1 \\ 0 & -\frac{f_v}{J_{eff}} \end{bmatrix} x + \begin{bmatrix} 0 \\ \frac{1}{J_{eff}} \end{bmatrix} u \\ y &= [1 \ 0]x \end{aligned} \quad (15)$$

In the next section, we have analyzed the stability of the pan mechanism.

B. Stability Analysis of Pan Mechanism

The stability analysis of the pan mechanism is based on its equilibrium points. For this purpose, we have found all the equilibrium points similar to section II (B). The equilibrium points are located at the $(x_1, 0)$ where x_1 belongs to the set of real numbers. Now we analyze the behavior of the pan mechanism at equilibrium points. Similar to (7), the function for the stability analysis of the pan mechanism based on (15) is presented here

$$f(x) = \begin{bmatrix} \dot{x}_1 \\ \dot{x}_2 \end{bmatrix} = \begin{bmatrix} x_2 \\ -\frac{f_v}{J_{eff}} x_2 \end{bmatrix}$$

The Jacobian at $(x_1, 0)$ of the pan mechanism is as follows

$$A = \left. \frac{\partial f}{\partial x} \right|_{(x_1, 0)} = \begin{bmatrix} 0 & 1 \\ 0 & -\frac{f_v}{J_{eff}} \end{bmatrix}$$

Using the values of f_v (0.007) and J_{eff} (0.4173) the expression above takes the following form

$$A = \begin{bmatrix} 0 & 1 \\ 0 & -0.01677 \end{bmatrix}$$

The eigenvalues are found as

$$|\lambda I - A| = \begin{vmatrix} \lambda & -1 \\ 0 & \lambda + 0.01677 \end{vmatrix} = \lambda^2 + 0.01677\lambda$$

$$\lambda^2 + 0.01677\lambda = 0, \lambda_{1,2} = 0, -0.01677$$

For the equilibrium points at $(x_1, 0)$ the eigenvalues are at 0 and -0.01677 . As one of the eigenvalues of A is zero, the phase portrait is in some sense degenerated. Therefore, matrix A has a nontrivial null space. All vectors in the null space of A are equilibrium points for the system. All the trajectories converge to the equilibrium subspace as $\lambda_2 < 0$. We have obtained results for the stability analysis of the pan mechanism similar to the stability analysis of the tilt mechanism.

C. Transfer Function of Pan Mechanism

The transfer function of the pan mechanism is determined using (15), value of f_v , table II and $G(s) = C(sI - A)^{-1}B$, and is given below

$$G(s) = \frac{2.3964}{s^2 + 0.01677s} \quad (16)$$

D. Pan Mechanism Response

Similarly, as noticed in [7,14], for (16) the setting time and steady-state error are 495 sec and 114.4994 respectively, when the gain (6.1118×10^5) is selected on the intersection of the root locus and the radial line. These values far exceed the desired performance values. This deficiency has to be compensated by designing the control system. The design of control system for the pan mechanism is explained in the next section.

V. MOTION CONTROL OF PAN MECHANISM

The linear pan mechanism is controlled by lead compensator to meet the desired conditions on the transient and the steady state response as shown in fig. 6. The compensated pan system (pan mechanism with lead compensator) analysis and simulation via the root locus method is presented here.

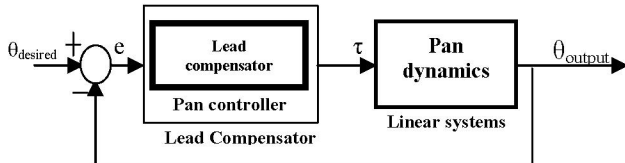


Fig. 6. Pan feedback control system

The objective of a lead compensator is to drive the T_s to less than 0.5 sec for the unity feedback system. The compensated system is schematically shown in fig. 6. The lead compensator

is found by using [9-12]. For the lead compensator, the calculated natural frequency, the desired dominant pole location (DPL) and zero location (z_c) are

$$w_n = 28.9855 \text{ rad/sec}, DPL = -20.00 + 20.9739 i, \\ \text{Angle at desired pole} = 92.2711^\circ, z_c = 0.01, \\ \text{Angular Contribution by zero} = -46.3471$$

Hence, the compensator angle contribution is 46.3818° and thus the lead compensator is

$$G_c(s) = \frac{s + 0.01}{s + 39.99} \quad (17)$$

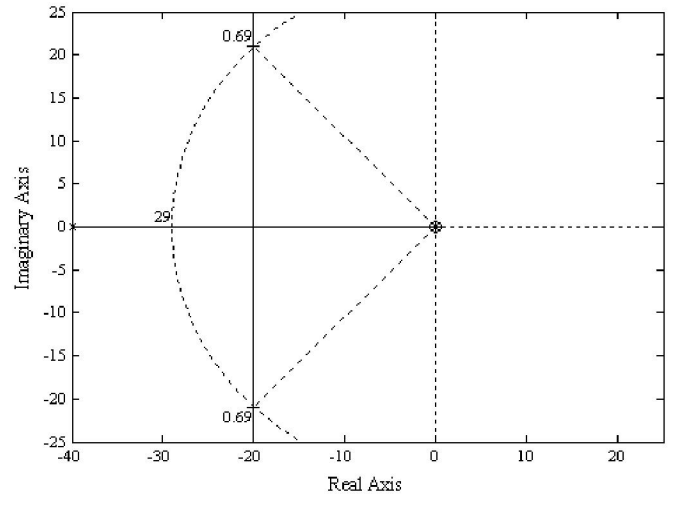
The open-loop transfer function resulting for fig. 6 is determined by using (16) and (17), and is given below

$$KG(s)G_c(s) = K \frac{2.3964(s + 0.01)}{s(s + 0.01677)(s + 39.99)} \quad (18)$$

The transfer function of pan system with lead compensator was determined in (18). According to the root locus technique [9], it has three branches of root locus, symmetrical with respect to the real axis, real-axis segment is $[0, -0.01]$ and $[-0.01677, -39.99]$, starting points are the open-loop poles at 0, -0.01677 and -39.99 , ending points are the open-loop zeros at $-0.01, \infty$ (∞), $-\infty$, real-axis intercept is at -19.9983 , angle of asymptotes are $90^\circ, 270^\circ$, breakaway point is at -19.9983 . The result of the root-locus method, based on simulation performed using Matlab is shown in fig. 7 (a) and (b).

A damping ratio of 0.69 is represented by a radial line intersecting the root-locus. We have found dominant pair of poles at $-19.9984 \pm 20.7298i$ along the damping ratio line for a gain (K) equal to 346.0983. The compensated system step response is shown in fig. 7 (b). The closed loop transfer function ($T(s)$) based on (18) is as follows

$$T(s) = \frac{848.9 s + 8.489}{s^3 + 40.01 s^2 + 849.6 s + 8.489} \quad (19)$$



(a)

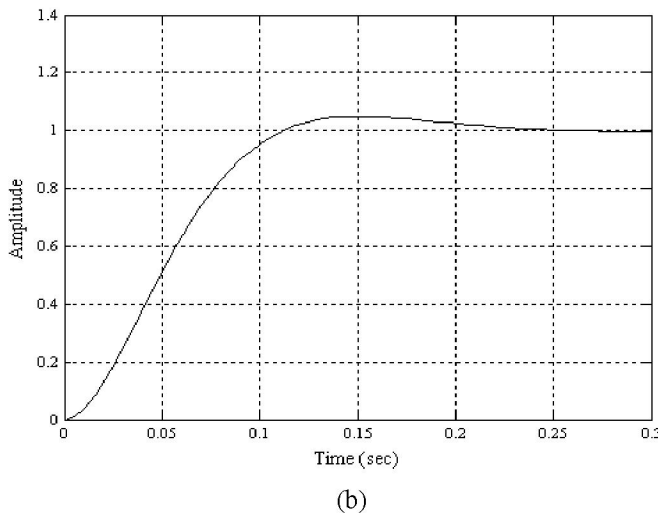


Fig. 7. Compensated pan system (a) root locus with radial line
(b) step response

As noticed in fig. 7(b), the setting time (0.207 sec) and the steady-state error (0.0809) meet the desired performance values.

VI. RESULTS

Linear modeling of the Tilt and Pan Mechanisms and its simulation based on feedback control system using the lead compensators for them leads to the desired results presented in the table III.

TABLE III
COMPENSATED SYSTEM MODEL RESULTS

	T_s (seconds)	e_{ss}	%OS
Tilt Mechanism	0.1960	0.7574	4.44
Pan Mechanism	0.2070	0.0809	4.79

In order that the steady state error and %OS do not increase more than desired values, encoder and Optoschmitt sensor are used in the real time system. The Optoschmitt sensor checks that %OS does not increase more than the desired value. The encoder attached with motor gives the position of motor shaft. The positioning accuracy of 0.0015 rad was achieved for the pan and tilt mechanisms. This was achieved by using the DC-motor having encoder of resolution 4096 pulses/revolution. This ensures the steady state error stays below the desired value (<2%).

Through analysis and simulation desired results were achieved. The model of the pan and tilt mechanisms with lead compensators gives us desired orientation of camera. This work is extendable and applicable to the mechatronic systems such as robotic arms and serial or parallel linked robotic mechanisms. Thus robotics system is worth for tracking systems.

VII. COMPARISON OF RESULTS

The linear models of the pan and tilt mechanism with lead compensators are compared with linear models of pan and tilt

mechanisms with PD controllers in [14]; comparison of the results is presented in table IV. It may be noted that

TABLE IV
COMPARISON OF RESULTS

	System with Lead Compensator			System with PD Controller		
	T_s (sec)	e_{ss}	%OS	T_s (sec)	e_{ss}	%OS
Tilt Mechanism	0.1960	0.7574	4.44	0.2068	2×10^{-4}	21.7
Pan Mechanism	0.2070	0.0809	4.96	0.1995	5×10^{-6}	21.5

- In terms of T_s both the compensated systems behave in similar manner. In terms of e_{ss} the PD controller gives better results.
- The linear models of the pan and tilt mechanism with lead compensator give better result in terms of %OS. This makes lead compensator a better option than PD controller.

ACKNOWLEDGMENTS

The authors are indebted to the National University of Sciences and Technology, Rawalpindi, Pakistan, the Pakistan Science foundation and the Higher Education Commission of Pakistan for having made this research work possible.

REFERENCES

- [1] R.J. Schilling, "Fundamental of robotics analysis and control", Prentice Hall, 1990.
- [2] Hassan K. Khalil, "Nonlinear system", Prentice Hall, 3rd edition, 2002, pp. 35 – 60.
- [3] John J. Craig, "Introduction to Robotics Mechanics and Control", Addison-Wesley, 3rd edition, pp. 153, 196-197, 2007.
- [4] C. D. Pollak and G. J. Thaler, "s-plane design of compensators for feedback systems," IRE Trans. Automat. Contr., vol. 6, September 1961 pp. 333 - 340..
- [5] Evans, W. R., "Control system synthesis by root locus method", AIEE Transactions, vol. 69, 1950, pp.547 – 551.
- [6] C. D. Pollak and G. J. Thaler, "s-plane design of compensators for feedback systems," IRE Trans. Automat. Contr., vol. 6, Sep 1961, pp. 333 - 340.
- [7] Imran S. Sarwar, Afzaal M. Malik, "Modeling, analysis and simulation of a Pan Tilt Platform based on linear and nonlinear systems", IEEE/ASME, China, Accepted, Oct 2008.
- [8] João B. Gonçalves^I, Douglas Eduardo Zampieri^{II}, "An integrated control for a biped walking robot", Journal of the Brazilian Society of Mechanical Sciences and Engineering, J. Braz. Soc. Mech. Sci. & Eng. vol.28 no.4 Rio de Janeiro, Oct./Dec. 2006.
- [9] Norman S. Nise, "Control systems engineering", Wiley student edition, Forth edition, pp. 515-524, 2004.
- [10] Jingrui Zhang^a, Shijie Xu^b, Junfeng Li^a, "A new design approach of PD controllers", Elsevier, Mar 2005, pp. 329–336.
- [11] Concepcion A. Monje, Vicente Feliu, "The Fractional Order Lead Compensator", IEEE, 2004.
- [12] William Messner, "The development, properties, and application of the complex phase lead compensator", Proceedings of the American Control Conference Chicago, Illinois, IEEE, Jun 2000.
- [13] Imran S. Sarwar, "Design, modeling and control of Pan Tilt Platform for unmanned aerial vehicle", M.S. thesis, Dept. Mechatronics Eng., NUST, Rawalpindi, Pakistan, 2006.
- [14] Imran S. Sarwar, Afzaal M. Malik, "Analysis and simulation of a Pan Tilt Platform based on linear model", NUST Journal, Accepted, 2008.
- [15] Katsuhiko Ogata, "Modern Control Engineering", Prentice Hall, 3rd edition, pp. 409 – 417.